Vol. 260: 83–96, 2003 | MARINE ECOLOGY PROGRESS SERIES
Mar Ecol Prog Ser | Published September 30

Lagrangian descriptions of marine larval dispersion

D. A. Siegel[1,*], B. P. Kinlan[2], B. Gaylord[3], S. D. Gaines[2,3]

[1]Insitute for Computational Earth System Science and Department of Geography, [2]Department of Ecology, Evolution and Marine Biology, and [3]Marine Science Institute, University of California, Santa Barbara, California 93106, USA

ABSTRACT: Many marine organisms are sedentary as adults and are redistributed between generations by the oceanic transport of planktonic larvae. In order to assess interactions among oceanographic and biological processes that determine larval dispersal patterns, we introduce a Lagrangian (or water-parcel-following) description of larval transport. This formalism is used to determine larval dispersal kernels (larval settlement probability distributions) for a range of ocean flows, planktonic larval durations and settlement pre-competency/competency periods. Paths of individual planktonic larval releases are modeled statistically and, by averaging over many individuals, ensemble estimates of larval dispersal are determined. Typical dispersal scales vary from a few km to >400 km. Modeled dispersal kernels are well explained using only a few readily available biological and oceanographic parameters, and derived dispersal scales agree well with population-genetic estimates, suggesting that the model has reasonable predictive power. An index for regional-scale self-seeding is presented, and is used as a tool to evaluate the efficiency of marine conservation areas. Finally, settlement patterns resulting from larval releases made over short times (days to months) should be comprised of a small number of discrete samples taken from the long-term averaged dispersal kernel. The resulting larval dispersal patterns will be quasi-random in both space and time, which will have important implications for the interpretation of settlement time series and the prediction of recruitment of sessile organisms.

KEY WORDS: Larval transport · Dispersal kernels · Coastal circulation · Larval dispersal distance · Marine protected areas · Planktonic larval duration · Self-seeding

INTRODUCTION

Understanding and predicting the spatial distribution of organisms is among the most fundamental goals of population ecology. This requires knowledge of both local processes leading to births and deaths, and non-local processes that redistribute organisms in space. In intertidal and subtidal marine environments, many species are sessile or highly sedentary as adults, with dispersal occurring predominantly during a planktonic larval stage. As a consequence, particularly for organisms with planktonic periods of days to months, oceanographic processes can play critical roles in the dynamics of populations (Jackson & Strathmann 1981, Roughgarden et al. 1988, Gaylord & Gaines 2000). Detailed numerical flow simulations and indirect measurements of dispersal ability have yielded insights into the movement of certain species of marine larvae in particular systems (Sammarco & Andrews 1988, Cowen et al. 2000). However, a general framework for predicting patterns of dispersal from simple biological traits and ocean flow parameters does not yet exist.

Estimates of dispersal scales can be made knowing characteristics of the oceanographic flow field and 2 fundamental biological variables: the length of time larvae spend in the plankton before they become developmentally and physiologically capable of settling (the pre-competency period), and the duration of time over which larvae can settle (competency period; e.g. Jackson & Strathmann 1981). These biological fac-

*Email: davey@icess.ucsb.edu

tors determine the period of time over which physical processes influence larval transport and, under the assumption that larvae act as passive particles, allow prediction of dispersion patterns. The result is a null model of larval transport incorporating only basic oceanography and the simplest biological parameters. Various factors, including larval behavior, timing of larval release, internal wave-driven transport, and local variations in Ekman transport, have all been implicated in influencing larval movement (see review by Shanks 1995). However, it remains unclear whether these processes simply introduce 'noise' around an overall template of larval dispersal set by oceanographic structure and the time course of larval settlement. As empirical data on marine dispersal distances emerge, comparison with a simple null model may highlight cases in which unique biological or physical processes, not captured in the simple model, play a role in larval dispersal.

An ideal null model of larval dispersal would both generate predictions that can be tested and provide the basis for incorporating empirical data into theoretical studies. Dispersal kernels provide a convenient way to do each by quantifying the average spatial distribution of larval settlers originating from a given point in space (e.g. Hastings & Higgins 1994, Botsford et al. 2001). This eliminates the need to track individuals (making the method well-suited for application with metapopulation models), while still allowing for comparison with empirical dispersal data from genetic or natural tagging estimates (Swearer et al. 1999, Kinlan & Gaines 2003, Palumbi 2003). Fundamental characteristics of dispersal, such as mean absolute displacement, the fraction of larvae arriving from a particular source, and the shape of the dispersal distribution, are all easily derived from the kernel descriptions.

Prediction of dispersal kernels requires knowledge of the spatial and temporal scales over which dispersal occurs and the scale-dependent processes regulating larval dispersal. Marine larval dispersal scales range from a few meters to 100s of kilometers (e.g. Scheltema 1971, Roughgarden et al. 1988, Botsford et al. 1994, Cowen et al. 2000, Kinlan & Gaines 2003). Estimates of average larval displacement are generally well correlated with corresponding planktonic larval durations (Fig. 1), although exceptions do exist (Shanks et al. 2003). In general, the longer the planktonic duration, the further larvae will disperse.

Dispersal scales, however, must also be viewed within the context of the substantial variability in flow that characterizes coastal circulation. The amplitude of the fluctuating components of velocity is, more often than not, larger than the time-averaged mean currents (e.g. Davis 1985, Poulain & Niiler 1989, Ohlmann et al. 2001, Poulain 2001). Typical root-mean square amplitudes of surface currents are generally many times larger than regional scale mean currents (e.g. Swenson & Niiler 1996, Dever et al. 1998). Hence, individual particle trajectories often bear little resemblance to the mean flow and can exhibit convoluted, seemingly chaotic paths. Examples of this arise in surface drifter trajectories from a variety of coastal regions, including the California Current (Davis 1985, Winant et al. 1999), the Gulf of Mexico (Ohlmann et al. 2001), and the Adriatic Sea (Poulain 2001). For similar reasons, individual larvae released from the same location at different times may ultimately find themselves at quite different destinations. Though some trajectories may lead far downstream from the parental location, others may not stray far from the spawning site. Still others may head upstream, opposing the mean flow. This intrinsic variability means that the description of mean larval dispersal requires an analysis of many larval trajectories through a variable flow field.

This concept of transport by means of quasi-random trajectories is subtly different from standard advection-diffusion approaches. In Fickian diffusion, net particle transport is strictly down-gradient due to the action of small-scale eddies (where 'small' is relative to the spatial scale of particle density). In turbulent coastal flows, the largest scales of motion are responsible for particle dispersal, and the movement of an individual water parcel is serially autocorrelated on the timescales of days. Traditional advection-diffusion approaches can

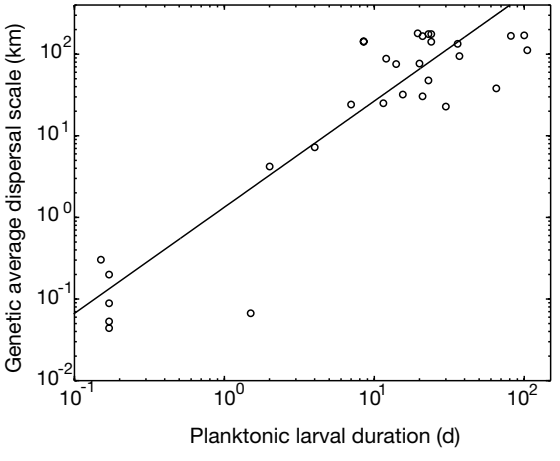

Fig. 1. Genetic estimates of mean absolute dispersal distance (D_d in km) vs mean planktonic larval duration (PLD in days) for 32 species (19 invertebrates, 12 fish, and 1 macroalgae) from a range of geographic locations and taxonomic groups (data from Kinlan & Gaines 2003). The complete data set with references is in Appendix 1, available at www.int-res.com/journals/suppl/siegel_appendix.pdf. Mean planktonic larval durations are estimated from larval otolith aging (fish) or laboratory culture studies (algae, invertebrates). The regression line is $D_d = 1.33\ (PLD)^{1.30}$ and the r^2 value for the fit is 0.802 (N = 32)

yield faithful results when evaluated over timescales of sufficient duration. However, these methods may not be useful on shorter timescales, as the short-time dispersal patterns act over relatively small spatial scales. In a turbulent ocean, long distance transport of larvae can occur on short timescales due to transport by the largest eddies in the flow. These differences, effectively between the concepts of stirring and mixing, are important and will be discussed later in the paper.

Here, we present a Lagrangian (water parcel following) simulation model of larval dispersion based on larval precompetency/competency periods and basic statistics of coastal oceanographic flow fields. Results of this model are used to derive dispersal kernels for larval transport under a wide range of flow scenarios. This null model of larval dispersion is confronted with empirical metrics of marine dispersal distances in order to illustrate the utility of merging theoretical and empirical dispersal estimates in a common framework. The present results are used to estimate an index for regional-scale self-seeding that is useful for evaluating the efficiency of a marine protected area. Finally, we address the role of temporal scale on predictions of larval transport.

MATERIALS AND METHODS

To assess larval dispersal in turbulent coastal flows, we apply a simple, stochastic method for simulating the trajectories of many planktonic individuals in a quasi-realistic velocity field. This approach has long been used to model dispersal of pollutants in the lower atmosphere (Hall 1975, Thompson 1984, Wilson & Sawford 1996) and has recently been applied to ocean flows (cf. Siegel & Deuser 1997, Bauer et al. 1998). The resulting particle trajectories are ensemble-averaged to yield a statistical description of the dispersal kernel, which can subsequently be parameterized for comparison with empirical estimates and used in population dynamic models.

Stochastic Lagrangian simulations are employed over a diffusion-based approach (e.g. Black et al. 1990, Possingham & Roughgarden 1990) because the simulation framework allows easy incorporation of, and comparison with, field observations. Specification of eddy diffusion coefficients requires either detailed field studies of dye or surface drifter dispersion (Okubo 1971, Poulain 2001, Sundermeyer & Ledwell 2001), or the results of a regional circulation model (Wolanski et al. 1989, Black et al. 1990). Each approach requires intensive efforts to determine eddy diffusivities and then with a poorly characterized understanding of uncertainty. The stochastic simulation method, in contrast, requires only a knowledge of statistics of the velocity field, which are comparatively easy to determine from field observations.

To simulate the movement of a larval 'particle' in a stochastically varying flow field, we implement a Markov chain model. At each time step, a particle updates its velocity by receiving a small random impulse. The resulting particle trajectory is similar to a random walk, except that the steps are serially autocorrelated. After some time, formally defined as the Lagrangian decorrelation timescale (τ_L), the motion of the particle becomes statistically independent from its previous motions. Trajectories of many, similar independent 'particles' are then simulated, enabling an estimation of relevant dispersion statistics.

Briefly, particle trajectories are simulated as follows: The alongshore position of the ith particle at time step n + 1, x_i^{n+1}, can be predicted knowing its previous position, x_i^n, the mean alongshore velocity of the flow field, U, and the fluctuating alongshore velocity acting on the particle, u_i^n, or:

$$x_i^{n+1} = x_i^n + \Delta t(U + u_i^n) \quad (1)$$

where Δt is the time step. A similar expression is used for cross-shelf position, y_i^n, and fluctuating velocity component, v_i^n. For the problems addressed here, flow statistics are assumed to be known and constant in time. The fluctuating component of current acting on particle i, u_i^n is altered each time step by a normal random deviate with an amplitude specified by the root mean square (rms) of the fluctuating currents, σ_u, or:

$$u_i^{n+1} = u_i^n\left(1 - \frac{\Delta t}{\tau_L}\right) + \sigma_u\sqrt{\frac{2\Delta t}{\tau_L}}\mathrm{RN} \quad (2)$$

where τ_L is the Lagrangian decorrelation timescale and RN is a random deviate selected from a normal distribution with unit variance and zero mean. A similar expression is used for the cross-shelf component, v_i^n. A new random deviate is selected each time step and the updated fluctuating current at the particle is used to advect the particle following Eq. (1). As the value of $\Delta t/\tau_L$ is small (typically 0.01 to 0.03), the effects of the random impulses are small for each time step and the particle retains most of its initial trajectory. After some time (approximately τ_L), the particle's motion will become independent of the value for the previous time step. Further information about this approach can be found in excellent reviews by Rodean (1996) and Wilson & Sawford (1996).

Five oceanographic parameters are important in this method for simulating individual particle trajectories in a hypothetical coastal ocean. These are: the mean velocity components, U and V, a measure of the amplitude of the fluctuating currents, σ_u and σ_v, and the Lagrangian decorrelation time, τ_L. Values of τ_L are typ-

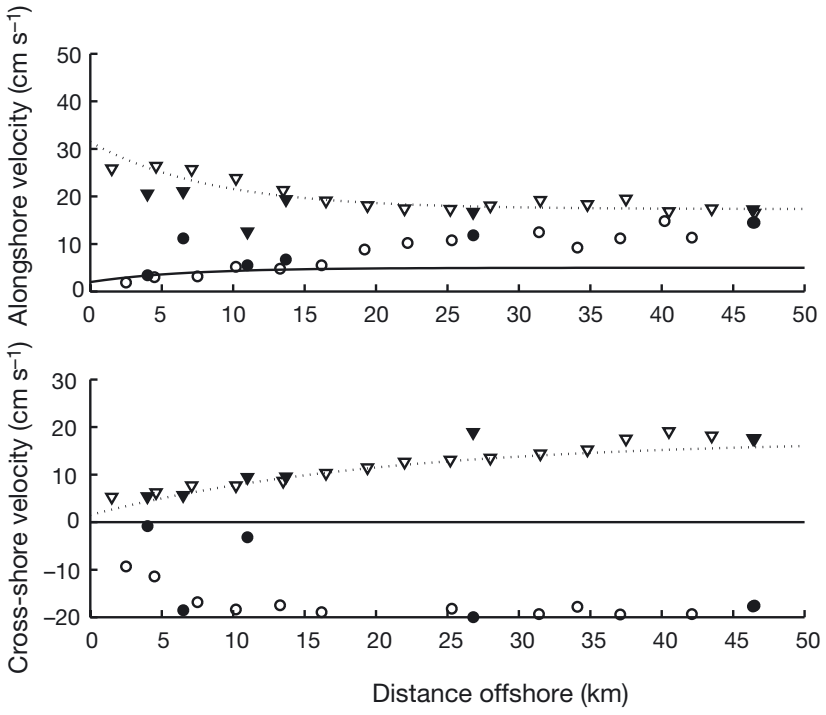

Fig. 2. Profile of alongshore (upper) and cross-shore (lower) velocity profiles used in the CODE-like scenarios. Observations are from Davis (1985) at the site of the Coastal Dynamics Experiment (CODE) just north of Pt. Arena, California, for the month of July 1982. Surface layer mean velocity determinations are denoted by circles and root mean square (rms) values by triangles. Observations from moored current meters are shown as filled symbols, and open symbols are from an analysis of drifter tracks. The solid and dotted lines give the profile used in the larval dispersion simulations of the CODE-like scenarios, i.e. $U(y) = 5 - 3\exp(-0.15y)$, $V(y) = 0$, $\sigma_u(y) = (300^{1/2}) + (200^{1/2})\exp(-0.12y)$, $\sigma_v(y) = (300^{1/2}) - (250^{1/2})\exp(-0.05y)$. All fits were done by eye. Positive alongshore current is taken to be southward in this depiction

ically 2 to 4 d for surface drifter observations from the coastal ocean (e.g. Davis 1985, Swenson & Niiler 1996, Brink et al. 2000, Poulain 2001). The Lagrangian decorrelation time is assumed to vary with distance offshore, ranging from 3 d far offshore, to ½ d at the coast, or:

$$\tau_L(y) = 3 - 2.5e^{-2y} \quad (3)$$

where y is the distance offshore (in km). This parameterization for τ_L is aimed to account for cross-shelf changes in the timescales of motion due to surface waves, tidal flows and so on, and its effects will be discussed below. Finally, a time step of 0.01 d is used.

For most of the simulations presented, the flow field is assumed to be vertically uniform (i.e. barotropic), the long-term mean cross-shelf current is zero (V = 0), and the fluctuating currents are symmetric (σ_u = σ_v), stationary (U and σ_u do not change with time) and homogeneous (U and σ_u do not change with location). Numerous flow scenarios are simulated in which mean currents range from 0 to 10 cm s^{-1} and fluctuating currents (standard deviations from the mean) range from 5 to 20 cm s^{-1} (both in increments of 5 cm s^{-1}). This results in 12 separate determinations of larval dispersal for any given larval competency time course, although some combinations of flow statistics are not realistic (cf. large U with small σ_u).

Coastal flows are rarely homogeneous, as fluctuating components of flow tend to follow lines of constant depth inshore and become more isotropic offshore. Surface drifter and moored current meter observations from the Coastal Dynamics Experiment (CODE) off the central California coast show that the fluctuating velocity component in the cross-shelf direction increases offshore, while the alongshore component decreases (Davis 1985, Fig. 2). These observations of inner-shelf exchange were made during summer and represent peak upwelling conditions in this eastern boundary current. The fluctuating components show the expected pattern of strong asymmetry onshore (σ_u ~ 30 cm s^{-1} and σ_v ~ 1.5 cm s^{-1} at the coastline) and approach a symmetric pattern offshore. The alongshore mean velocity increases offshore to a maximum value of ~10 cm s^{-1}, while the mean crossshore velocity increases from 0 to ~20 cm s^{-1} in the offshore direction. We use these data to derive a 'CODE-like' heterogeneous flow scenario for comparison with the homogeneous flow simulation results (Fig. 2). Although the CODE results show an alongshore mean flow which increases offshore (Fig. 2), conservation of mass requires that the mean cross-shelf flow be set to zero. Implications of this and other assumptions are discussed below.

A correction is required when this stochastic simulation method is applied to inhomogeneous flow fields, as particles collect in low-speed regions of the flow (e.g. Thompson 1984). This violates the well-mixed hypothesis, which states that a uniform particle distribution should remain uniformly distributed as long as there are no convergences or divergences (Thompson 1987). First-order correction terms for the well-mixed hypothesis have been proposed (e.g. Rodean 1996, Wilson & Sawford 1996) which account for the change in velocity variance in the offshore direction, or:

$$v_I^{n+1} = v_I^n\left(1 - \frac{\Delta t}{\tau_L}\right) + \sigma_u\sqrt{\frac{2\Delta t}{\tau_L}}RN + \frac{\Delta t}{2}\left(1 + \left(\frac{v_I^n}{\sigma_u}\right)^2\right)\frac{\partial(\sigma_u)^2}{\partial y} \quad (4)$$

No correction is needed in the along-shelf direction. The last element required is the larval pre-competency/competency time course. Average planktonic larval durations can range from an hour to several months, depending on the organism in question (see Fig. 1). In our simulations, larvae are released near a single linear coastal boundary, and only those individuals that return to the coastline during their competency interval are allowed to settle. Those that encounter the shoreline during their precompetency period remain in the plankton, whereas those that do not reach the coast by the end of the competency period perish. We use 5 larval precompetency/competency time courses (0 to 5, 6 to 12, 14 to 21, 24 to 36 and 42 to 56 d). Longer competency windows are needed for longer precompetency times to ensure that an adequate number of simulated settler trajectories are sampled (this increase in competency period with mean time in the plankton is also biologically realistic; see Wellington & Victor 1989). However, this choice does impact the fraction of released larvae that do settle. A total of 65 different simulations are conducted (13 flow scenarios and 5 larval time courses).

The dispersal kernel, $K_{x-x'}$, is defined as the density of settling larvae at X′ (no. km^{-1}), normalized by the number of settlers released from Location X. Dispersal kernels are estimated by calculating the density distribution of settlers based on many individual releases from a single location. The integral of a dispersal kernel over all space is equal to 1. For the calculations presented here, kernel functions are determined by ensemble averaging over at least 5000 individual trajectories. Dispersal kernels calculated in this way account only for those larvae that successfully settle. Most spawned larvae do not reach the shoreline during their competency window and perish (e.g. Roughgarden et al. 1988). In addition to intrinsic demographic factors such as predation or starvation, these 'fluid mechanical losses' can be a significant fraction of the total losses of larvae during the planktonic period (see 'Results').

The model presented here is aimed at approximating the mechanics of larval transport in a coastal ocean. It assumes that larvae are purely planktonic and are advected like passive particles. Its present implementation is simplistic, although it can, in principle, be extended to include detailed biological factors (i.e. organism behavior) and physical oceanography (i.e. detailed flow-field characteristics).

RESULTS

Example trajectories for larvae that can settle immediately and can remain in the plankton for up to 5 d (short planktonic larval duration [PLD] larvae), and larvae that can survive in the plankton for up to 8 wk after a 6 wk precompetency period (long PLD larvae), are shown in Fig. 3. A mean alongshore current of 5 cm s^{-1} and a fluctuating component of 15 cm s^{-1} is used. For both cases, particles show both downcurrent (to the right) and upcurrent trajectories. There appear to be more downcurrent trajectories than upcurrent ones, but the difference is subtle in this sample of 10 paths. Further, only a couple of larvae appear to settle during the assumed competency windows.

The large differences in spatial scale of dispersion between the 2 examples are of greater importance. This is a consequence of the 10-fold differences in their planktonic larval durations. Typical dispersion scales for the short PLD case are 20 to 40 km, whereas the long PLD larvae are typically found more than 200 km from their source (Fig. 3). Further, the long PLD trajectories are more convoluted than the short PLD paths. This is because the long PLD larvae are in the plankton much longer than typical Lagrangian decorrelation times ($\tau_L \leq 3$ d), and are thus subject to many independent fluctuations in the flow field. In contrast, each short PLD larval trajectory is constructed from just a few independent degrees of freedom.

Ensemble averaging over many individual trajectories enables calculation of the larval dispersal kernel, K_x. Dispersal kernels for short PLD and long PLD larvae are shown in Fig. 4. As hinted in Fig. 3, the most probable location of settlement (the mode of the distribution) occurs downstream of the spawning location. For short PLD larvae, the mode is only a short distance from the source, whereas for long PLD larvae, the mode is found >200 km downstream (Fig. 4). This reflects increasing advection by the mean flow with increasing time in the plankton. The half-height widths of the K_x distributions are ~40 km for the short PLD larvae and ~500 km for the long PLD larvae. This reflects variation in the effects of dispersive processes

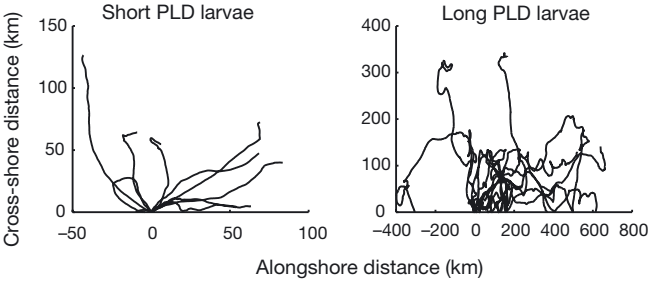

Fig. 3. Example trajectories for short (left) and long (right) planktonic larval duration (PLD) larvae in a flow with mean alongshore current of 5 cm s^{-1} and fluctuating components of 15 cm s^{-1}. Ten trajectories are shown for each type of settler. Mean flow goes from left to right. Short PLD larvae trajectories are plotted for 0 to 5 d while for long PLD larvae they are plotted from 0 to 56 d

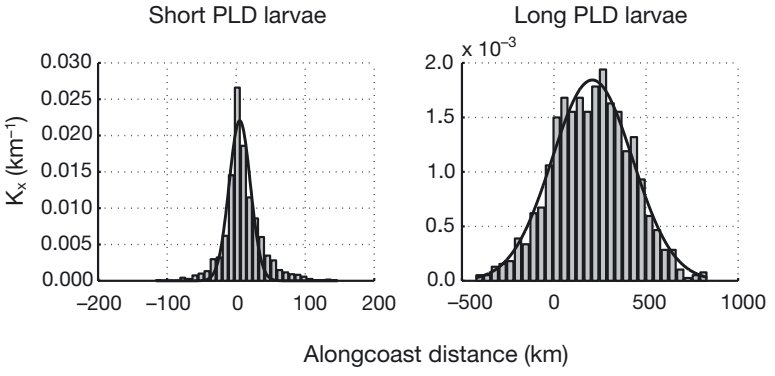

Fig. 4. Example kernel distributions for short (left) and long (right) planktonic larval duration (PLD) larvae in a flow with mean alongshore current of 5 cm s^{-1} and fluctuating components of 15 cm s^{-1}. Numerical simulation results are shown by vertical bars; Gaussian fits (Eq. 5) are shown by solid lines. Fit parameters are $K_o = 2.2 \times 10^{-3}$ km^{-1}, $x_d = 5.2$ km and $\sigma_d = 15$ km for the short PLD larvae case and $K_o = 1.84 \times 10^{-3}$ km^{-1}, $x_d = 208$ km and $\sigma_d = 219$ km for the long PLD case. Fits were excellent ($r^2 = 0.983$ and 0.990, respectively). Five thousand independent trajectories were used to construct the kernel functions; 1379 and 922 synthetic larvae settled for the short and long PLD larvae cases, respectively

over the 10-fold differences in the time these larvae spend in the plankton.

The dispersal kernels appear to be similar to a Gaussian distribution, which suggests their modeling using a compact form:

$$\hat{K}_x = K_o \exp\left(\frac{-(x - x_d)^2}{2\sigma_d^2}\right) \quad (5)$$

This results in 3 parameters for K_x: amplitude, K_o, downstream drift, x_d, and spread, σ_d. As the integral of K_x over all space is by definition equal to 1, only 2 of these parameters are unique (theoretically $K_o = 1/[(2\pi)^{1/2}\sigma_d)]$. A Gaussian distribution is chosen because it fits the observed K_x distributions well and it provides a link to traditional advection-diffusion approaches. Gaussian fits are performed on all 65 numerical experiments. Generally, least-square fits using the Gaussian model were excellent ($r^2 > 0.95$ for nearly all cases). The only exception was a short PLD case where the mean flow was greater than the root mean square of the fluctuating components ($U = 10$ cm s^{-1} and $\sigma_u = 5$ cm s^{-1}). This is not a concern, since this flow configuration is exceptional. A Gaussian model may not be the best analytical form for all applications. In particular, simulation results predict leptokurtic dispersal kernels for organisms with planktonic durations similar to the Lagrangian decorrelation timescale. This detail may not be important for modeling demographic connectivity among established populations, but could be critical for modeling of species invasion and colonization rates (e.g. Cain et al. 2000).

The role of flow configuration on the kernel fit parameters, as well as the fraction of released larvae that settled during the assumed competency window, are shown in Fig. 5 for the short PLD case and in Fig. 6 for the long PLD case. For both cases, the kernel spread (σ_d) increases and the kernel amplitude (K_o) decreases with increasing fluctuating current amplitude (σ_u). The kernel drift (x_d) is largely a function of the mean current (U). Distributions for other larval competency time courses support these generalizations (not shown). There are exceptions to these trends, particularly for short PLD cases at low σ_u values.

Approximately 1/4 of the total number of released particles settle during their prescribed competency windows for both the short and long PLD cases (Figs. 5 & 6). The remaining larvae are lost. These estimates of the fraction of settling larvae do not consider the many demographic processes (predation, starvation, etc.) that contribute to larval mortality. There are few significant changes in the fraction of settling larvae with flow parameters (see below).

The CODE-like flow scenarios allow us to assess the importance of flow-field homogeneity on the dispersal kernel. The CODE-like simulations use the flow field

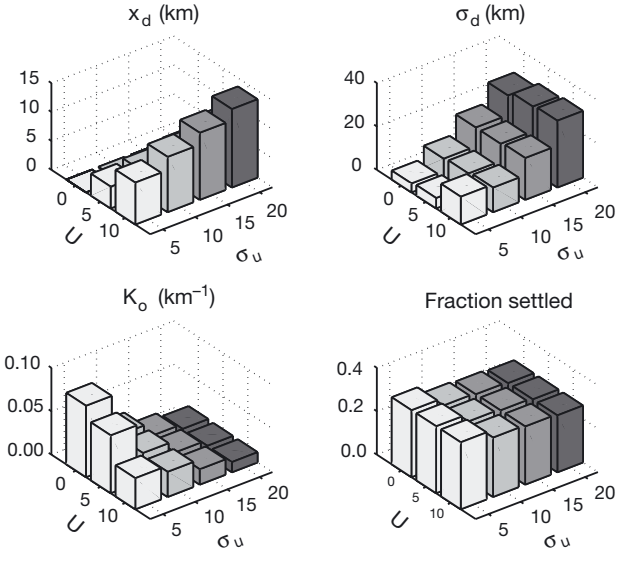

Fig. 5. Role of homogeneous flow field configuration on kernel fit parameters for the short planktonic larval duration (PLD) larvae case. Upper left panel: Kernel drift, x_d, as a function of U and σ_u in km. Upper right panel: Kernel spread, σ_d, as a function of U and σ_u in km. Lower left panel: Kernel amplitude, K_o, as a function of U and σ_u km^{-1}. Lower right panel: fraction settling larvae to total spawned larvae as a function of U and σ_u

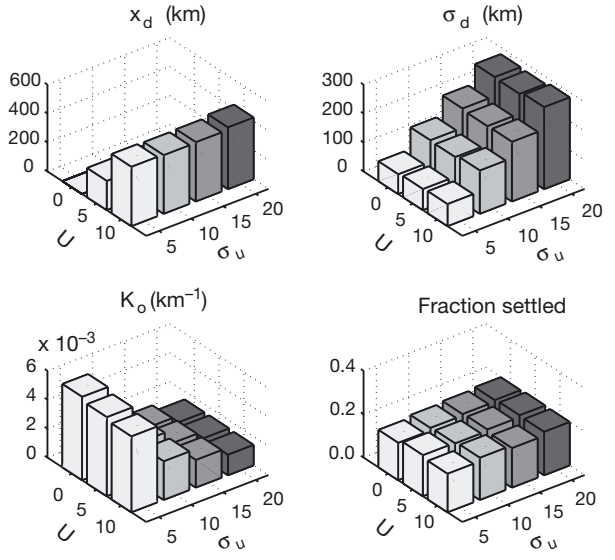

Fig. 6. Role of homogeneous flow field configuration on kernel fit parameters for the long planktonic larval duration (PLD) larvae case. Upper left panel: Kernel drift, x_d, as a function of U and σ_u in km. Upper right panel: Kernel spread, σ_d, as a function of U and σ_u in km. Lower left panel: Kernel amplitude, K_o, as a function of U and σ_u km^{-1}. Lower right panel: fraction settling larvae to total spawned larvae as a function of U and σ_u

given in Fig. 2 for 10 000 individual larval releases and apply the correction to enforce the well-mixed criterion (Eq. 4). Fig. 7 shows the resulting K_x fit parameters for the CODE-like flow field as a function of the mean time in the plankton for settled larvae (T_m). Also shown are results for a similar homogeneous case (U = 5 cm s^{-1} and σ_u = 15 cm s^{-1}). To first order, Gaussian fit parameters from the CODE-like (circle symbols) and the corresponding homogeneous (asterisk symbols) case are very similar. As expected, values of σ_d and x_d both increase with increasing T_m, and a large degree of quantitative similarity between the 2 kernel fit values is observed. This suggests that knowledge of spatial gradients of the flow field may be less important than the magnitude of the large-scale circulation and the average time an organism spends in the plankton.

Large differences in the fraction of released larvae that settle within their competency time periods are found between the homogeneous and inhomogeneous flow cases (Fig. 7). Only ca. 4% of the larvae settle in the CODE-like flow field, whereas ~20% of the released larvae settle in the homogeneous cases. This difference is likely due to the flow inhomogeneity correction (Eq. 4), which acts to push particles offshore from low- to high-speed regions of the fluid. The implications of this result and its robustness will be discussed below.

Fit values for the kernel parameters show a strong dependence on flow parameters for a given larval competency timeline (Figs. 5 & 6). Likewise, for a single flow field, the K_x parameters illustrate the importance of temporal details of the competency window parameters (Fig. 7). These clues can be used to devise a scheme for collapsing these parameters into a unified framework. It seems reasonable that the longer an organism is in the plankton, the further downstream it will be advected by the mean flow. Thus, one would expect that the kernel drift parameter (x_d) could be modeled as the product of the mean current (U) and mean time that individuals have been in the plankton (T_m). Using the database of kernel parameters, least-squares regression can be used to derive relationships between flow and larval settlement parameters (Fig. 8, Table 1). All experiments performed (N = 65) are used in these fits.

Retrieved values of the kernel drift (x_d) are accurately modeled using the mean current (U) and mean time an individual is in the plankton (T_m), as expected (Fig. 8). The fit coefficient between x_d and U T_m is nearly equal to 1, and this regression explains nearly all of the variance in x_d (Table 1). Following this logic, estimates of the kernel spread (σ_d), a result of turbulent mixing processes, should scale as the square root of the product of the fluctuating current variance (σ_u^2)

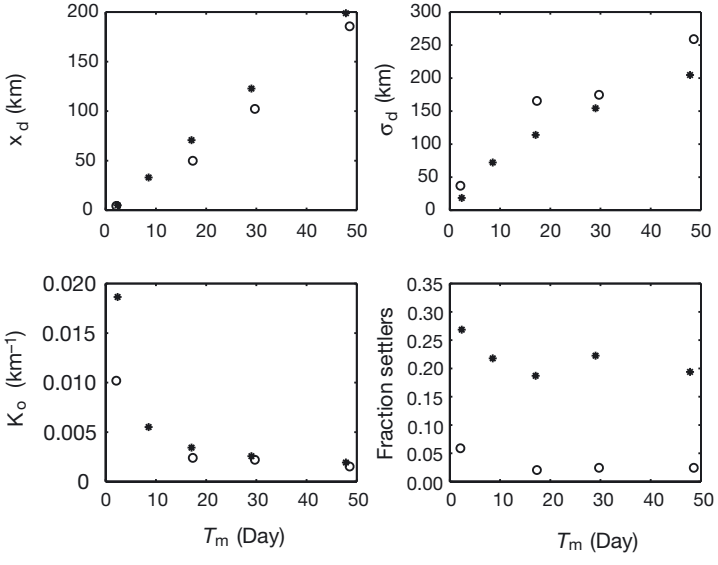

Fig. 7. Kernel fit parameters from the CODE-like flow field (o) and a corresponding homogeneous * case (U = 5 cm s^{-1}, σ_u = 15 cm s^{-1}) as a function of mean planktonic larval duration (T_m). Upper left panel: Kernel drift, x_d, vs T_m. Upper right panel: Kernel spread, σ_d, vs T_m. Lower left panel: Kernel amplitude, K_o, vs T_m. Lower right panel: ratio of settled larvae to total spawned larvae vs T_m

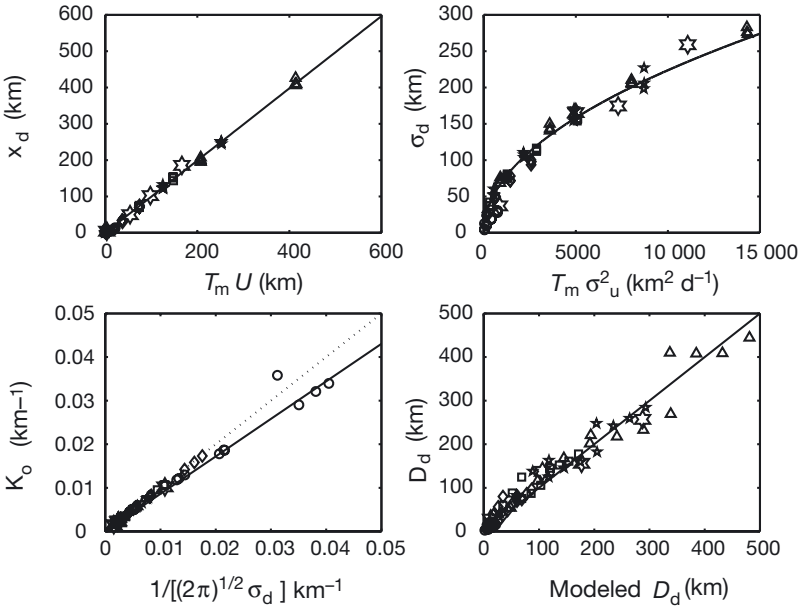

Fig. 8. Parameterization of kernel fit parameters x_d (upper left panel) and σ_d (upper right panel) as functions of mean planktonic larval duration (T_m) and flow parameters (U and σ_u) and K_o (lower left panel) as a function of σ_d. Shown in the lower right panel are simulated and regression-fit mean displacement, D_d, estimates. For the homogeneous flow scenarios, settling competency time courses are 0 to 5 d (○), 6 to 12 d (◇), 14 to 21 d (□), 24 to 36 d (☆) and 42 to 56 d (△). The large 6-pointed star symbols are results from the CODE-like flow field. Regression lines and statistics for the fits are given in Table 1. The dotted line in the lower left panel assumes a 1:1 relationship between K_o and $1/[(2\pi)^{1/2}\sigma_d]$, while the solid line is the fit relationship. For the simulated vs regression-modeled D_d estimates, a 1:1 line is plotted

and T_m (Fig. 8). Fit results are excellent for σ_d, explaining nearly 98% of the variance (Table 1). Following theory, Gaussian kernel amplitude (K_o) is a simple function of kernel spread (= $1/[(2\pi)^{1/2}\sigma_d]$; Fig. 8). Deviation in the fit parameter for K_o from 1 (Table 1) is driven by a few unusual flow scenarios ($\sigma_u/U <$ 1), and a value of 1 should be used in applications. In all, the parameters needed to quantify dispersal kernels are simple functions of a few flow parameters and the mean planktonic larval duration, suggesting this approach can be applied across a broad array of scenarios.

Table 1. Fit expressions for dispersion kernel parameters. Regression lines are shown in Fig. 8. Units are U (km d^{-1}), σ_u (km d^{-1}) and T_m (d). It is recommended that K_o be calculated using $1/[(2\pi)^{1/2}\sigma_d]$, with σ_d modeled as above, as a few exceptional cases are driving the regression parameter from 1

Kernel parameter	Fit relationship	r^2 of fit
Amplitude, K_o (km^{-1})	$0.861/[(2\pi)^{1/2}\sigma_d]$	0.991
Drift, x_d (km)	$0.994\,T_m U$	0.997
Spread, σ_d (km)	$2.238\,\sigma_u T_m^{1/2}$	0.979
Mean absolute displacement, D_d (km)	$0.695(T_m U) + 0.234(T_m \sigma_u)$	0.958

The mean absolute displacement of settlers, D_d, is a useful index for how fluid motions disperse larvae in their planktonic phase, and provides a mechanism for comparison with standard ecological metrics of dispersal distance. D_d can be formally defined in terms of the dispersal kernel as:

$$D_d = \int_{-\infty}^{\infty} |x| K(x)\,dx \quad (6)$$

For cases where $x_d = 0$, D_d is equal to $(2/\pi)^{1/2}\sigma_d$. Values of D_d are calculated numerically using the Gaussian-fit relationships (Eq. 5) and estimates vary from a few km to more than 400 km (Fig. 8). Mean absolute displacement is a function of both mean flow and dispersion by fluctuating components of flow, as illustrated by regression models (Table 1).

DISCUSSION

Several generalizable results emerge from the present Lagrangian simulation model of planktonic larval dispersal. First, predictions of larval dispersal can be developed from knowledge of the mean and fluctuating components of flow, coupled with basic information about an organism's larval competency time course. Second, expected dispersal scales range from less than 1 to more than several hundred kilometers, depending on these characteristics. Last, parameterizations for dispersal kernels can be derived using readily available flow and organism life-history characteristics. In the following sections, we evaluate validity bounds of the present modeling assumptions and compare the present results with empirical estimates of mean absolute displacement, D_d, derived from population genetic data. Model results are then used to provide insights into the prediction of regional-scale self-seeding for marine populations and the role of temporal scale in interpreting patterns of larval dispersion and recruitment.

Issues in the modeling of larval transport

The goal of this work is to best encapsulate the fundamental processes regulating larval dispersal into a simple, yet generally applicable, model of larval trans-

port. In attempting to achieve this goal, many issues have been ignored. This results in a 'null model' for larval transport that lies somewhere between a detailed simulation and a cartoon. Here, we discuss implications of the assumptions used and suggest directions for future work.

First, the basic underlying assumptions of a straight coastline and uniform alongshore flow statistics have a major influence on the types of processes that can be simulated. These assumptions were selected to best generalize results for a wide application. This means that persistent flow features, such as topographically induced recirculations, are not considered, although these processes can have a large influence on larval settlement patterns (Wolanski & Hamner 1988, Gaylord & Gaines 2000). As the fluctuating current fields are modeled as random variables, consistent temporal changes in mean currents, such as a tidal or seasonally reversing current, are not considered. These and similar issues could be easily modeled, although this would defeat our goal of creating a generalizable, null model.

Second, the assumption of alongshore flow uniformity limits the types of mean flows that can be modeled due to the mass conservation constraint and the assumption that motions are vertically uniform (see below). This requires that the mean flow remain constant over the alongshore scales modeled ($\partial U/\partial x = 0$), although cross-shelf changes in the along-shelf mean current can be considered. Further, the mean flow must be a spatial as well as a temporal mean. Regional-scale, temporal mean currents are typically small (often vanishingly small) as they average together conflicting currents from various locations and times. The appropriate spatial scale for current averaging is related to the scale over which larval dispersal occurs. Larvae with longer plankton durations require mean currents to be considered over larger spatial scales. For most situations, this means that the appropriate mean currents should be smaller than that for shorter PLD larvae.

Third, the flow field is assumed to be constant with respect to depth. Mass conservation considerations then require the cross-shelf mean flows to be zero ($V = 0$). This means that important potential larval delivery processes, such as internal waves, surface gravity waves, Ekman transport, bottom friction, and interactions with small-scale bathymetric features, are not considered. Vertical structure in the mean flow is needed to model interactions between flow and organism behavior, such as vertical migration. This could be done given appropriate mean and fluctuating current fields (but with a substantial loss of generality).

Fourth, the choice of Lagrangian decorrelation time (τ_L; Eq. 3), has some bearing on the modeling results. Experimentation with a variety of τ_L parameterizations results in few changes for the long PLD case, but some differences are found for the short PLD case (not shown). For the short PLD case, changes in the offshore τ_L profile cause small differences in the resulting kernel distributions (amounting to <4 km for x_d and <10 km for σ_d, compared with the case shown in Fig. 4). Further, a greater fraction of short PLD larvae settle as the value of τ_L is decreased. This sensitivity to the τ_L parameterization for the short PLD case makes sense as the PLD and the value of τ_L are roughly equivalent, and few independent degrees of freedom contribute to an individual larval release's trajectory. The long PLD case is rather insensitive to the choice of the τ_L parameterization, as many degrees of freedom contribute to individual trajectories. Overall, the present results are less reliant on the details of the parameterization of τ_L than on the other flow and biological parameters.

Fifth, the choice of larval precompetency/competency time course appears to have little influence over the characteristics of a larval dispersion kernel. The larval competency timecourse will have an important role in predicting the fraction of released larvae that successfully settle. That is, the longer the time over which settlement can occur (the competency time window), the greater the chance that a planktonic larva will settle, whereas the longer the precompetency timescale, the lower this probability will be. The present modeling assumes that the duration of the competency window increases with precompetency time. This is done to ensure that an adequate number of simulated settler trajectories are sampled, although there is biological justification for this assumption (e.g. Wellington & Victor 1989). For the homogeneous flow scenarios and larval competency time courses used, there are few significant differences in the fraction of released larvae that settles (Figs. 5 & 6). However when the CODE-like flow field is used, this fraction is much smaller (~4 vs ~20% for the homogeneous flows; Fig. 7), as it appears that the flow inhomogeneity correction (Eq. 4) acts to push particles offshore. The present experiments are clearly inadequate for addressing 'fluid mechanical' larval losses, and more detailed experimentation is needed. The resolution of this issue will be important for understanding life history tradeoffs and population persistence, where the balance between mortality and larval recruitment play critical roles.

Last, the null model of larval transport described here ignores several potentially important biological factors. For example, larvae are treated as surface-following, passive particles, which may not be true, particularly in their later stages of development. Many larvae migrate vertically to take advantage of different portions of the current profile, or physical features such as fronts and internal waves, leading to increased

or decreased dispersal (Hill 1991, Shanks 1995). The timing of larval release may correspond with non-random aspects of flow (e.g. Richards et al. 1995). Planktonic mortality may vary as a function of offshore distance. All of these factors are difficult to assess, and further experimentation (both field and numerical) is required. Nevertheless, a consideration of the potential biological complications first depends on the development of an appropriate null model. More complex biological and physical processes should be examined as deviations from this basic template.

Experimental verification of the dispersion kernel

Model predictions of average dispersal distance (D_d) are confronted with empirical estimates of larval dispersal derived from population-genetic data (Kinlan & Gaines 2003, Palumbi 2003). Demographic rates of dispersal can be estimated from the decrease in correlation of allele frequencies with distance (e.g. Wright 1943, Palumbi 2003). Genetic dispersal estimates reflect long-term average patterns of dispersal, as genetic correlations accumulate over hundreds of generations. Moreover, genetic estimates reflect only dispersal of propagules that successfully establish and reproduce (i.e. effective dispersal). Estimates of dispersal make assumptions about the distribution of effective dispersal in space, effective size of populations, and the spatial arrangement of subpopulations (Slatkin 1987). We used estimates of average dispersal distance derived from simulations assuming an exponential dispersal kernel, effective population size of 1000, and a 1-dimensional array of equally spaced subpopulations (Palumbi 2003). Sensitivity to both the assumptions used and the inherent accuracy of genetic data results in probable uncertainty levels for D_d estimates of less than a factor of 10 (Kinlan & Gaines 2003). However, the strong correlations of genetic D_d estimates with life-history proxies of dispersal ability (Fig. 1) suggest this uncertainty is likely less than the stated upper bound, perhaps a factor of 4 to 5 (B.P.K. & S.D.G. unpubl. data)

We identified 32 marine species (19 invertebrates, 12 fish, and 1 macroalga) for which both genetic estimates of D_d and estimates of planktonic larval duration were available (Fig. 1). These species are drawn from a variety of geographic areas and taxonomic groups. Mean planktonic larval duration was estimated from published larval otolith aging (fish) or laboratory culture results (invertebrates, algae). We compared genetic estimates of mean dispersal distance with model predictions of D_d (based upon the regression in Table 1) for the same species (Fig. 9). This is clearly not a direct comparison, as there are no oceanographic data associated with the genetic dispersal observations. Flow directionality is ignored, a reasonable assumption over the large spatial and temporal scales inherent in the genetic method, and a reasonable range of fluctuating current levels (5 cm $s^{-1} \leq \sigma_u \leq$ 15 cm s^{-1}) is assumed. Within the discussed uncertainty bounds, the null model estimates of D_d provide a reasonably good overall fit to genetic estimates (Fig. 9); points are roughly distributed about the 1:1 line.

Even allowing for uncertainty about oceanographic structure, some of the very long- and very short-dispersing species appear to provide hints of deviations from the null model (Fig. 9). Model predictions match genetic dispersal distances best at low fluctuating velocities (σ_u = 5 cm s^{-1}) for the short PLD larvae, and at higher fluctuating velocities (σ_u = 10 to 15 cm s^{-1}) for long PLD larvae. Deviations from model predictions at the extremes may be due to systematic differences in life-history strategies of organisms with divergent planktonic durations. Very short dispersers may not spend their full development time in the plankton, leading to shorter dispersal distances than predicted from the duration of the larval period. Some of the longest-dispersing species may be capable of delaying metamorphosis and remaining in the plankton longer than laboratory culture studies suggest, or may have behaviors that enhance dispersal. The use of a simple null model of dispersal assists in identifying when biological processes may modify dispersal distances. The

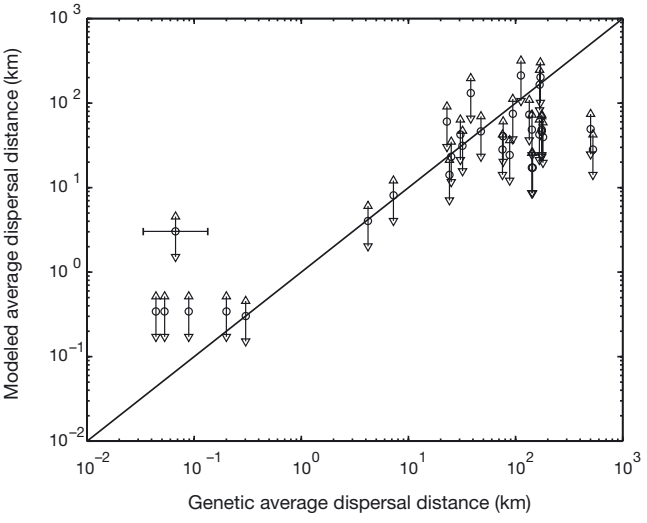

Fig. 9. Modeled mean absolute displacement (D_d) vs estimates of D_d derived from population-genetic data (from Kinlan & Gaines 2003). The genetic data used here are the same as in Fig. 1. Modeled estimates of D_d use the expression derived in Table 1 with U = 0 cm s^{-1} and σ_u = 5, 10 and 15 cm s^{-1} (the symbols ∇, ○ and △, respectively). Uncertainties in the genetic dispersal estimates are thought to be a factor of 4 to 5 and an example of this range is shown on the left portion of the figure (see text for details). A 1:1 line is plotted

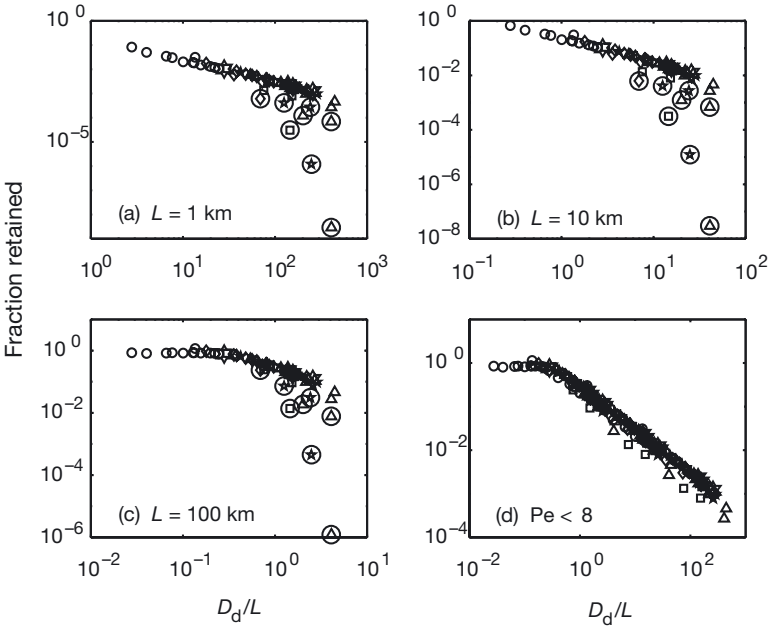

Fig. 10. Regional-scale larval self-seeding as a function of the ratio of the absolute dispersal scale (D_d) to the length scale of the region of interest (L). Length scales of (a) 1, (b) 10 and (c) 100 km are used, and these results are combined in Panel (d). In the Panels (a) through (c), cases where the Peclet number (Pe) is greater than 8 are circled and these cases are not considered in Panel (d). As before, settling competency time courses are 0 to 5 d (○), 6 to 12 d (◇), 14 to 21 d (□), 24 to 36 d (☆) and 42 to 56 d (△) for the homogeneous flow field, and the larger 6-pointed star symbols are results from the CODE-like flow

utility of such comparisons will increase as new techniques, such as analysis of natural microchemcial tags (Swearer et al. 1999), provide more precise and frequent estimates of larval dispersal properties.

Larval self-seeding in a null model

Understanding the degree to which local populations are seeded by their own larvae is essential to effective management of marine populations, and has become the subject of much recent attention (e.g. Roberts 1997, Swearer et al. 1999, Cowen et al. 2000). An objective measure of larval self-seeding can be made by calculating the fraction of total settling larvae that have settled within a region of extent, L, about their release location, or:

$$\text{Self}-\text{Seeding fraction} = \int_{-L/2}^{L/2} K(x)\,dx \qquad (7)$$

A value of 1 for the self-seeding fraction (SSF) indicates that the all-released larvae settle within a distance $L/2$ of their release point. Values of SSF depend on the relationship between the assumed regional scale (L) and the absolute larval dispersion scale (D_d). When D_d/L is small ($D_d/L < 1$), the self-seeding fraction should approach 1, as most larvae disperse at scales smaller than the region of interest. If D_d/L is much greater than 1, the fraction of released larvae that settle within the region should be small.

Estimates of the self-seeding fraction based on our model scenarios vary from nearly 1 to values as small as 10^{-9} (Fig. 10). As expected, smaller SSF estimates are found when smaller values of L are assumed (Fig. 10a–c). When L is set equal to 100 km, values of the self-seeding fraction approach 1 for many of the flow fields and planktonic larval durations investigated (Fig. 10a). However, if L is chosen to be 1 km, SSF values reach a maximum of ~0.1 and are often much smaller than this factor.

For each of the assumed L-values used, a handful of self-seeding fraction estimates depart from the rest of the simulated results (Fig. 10a–c). These SSF estimates correspond to flow regimes with relatively large mean flow values. The relative effects of mean and fluctuating components of flow on dispersion can be quantified using the Peclet number (Bird et al. 2001). The Peclet number is defined as the square of the ratio of the mean flow advection length scale (UT_m) to a diffusive length scale [$(\kappa T_m)^{1/2}$], or:

$$Pe = \left(\frac{\text{advective scale}}{\text{diffusive scale}}\right)^2 = \frac{(UT_m)^2}{\kappa T_m} = \frac{U^2 T_m}{\kappa} \qquad (8)$$

where κ is the eddy diffusion coefficient ($m^2\ s^{-1}$) which quantifies the rate of mixing due to turbulent ocean processes. Large values of the Peclet number indicate that mean flow advection dominates, whereas small values imply that the fluctuating components of flow are the most important. Following standard turbulence scaling, we model the eddy diffusion coefficient as the product of the fluctuating velocity variance, σ_u^2, and a mixing timescale, τ ($\kappa \sim \sigma_u^2 \tau$). Equating the mixing timescale with the Lagrangian decorrelation timescale, τ_L, a simplified expression for the Peclet number can be derived:

$$\text{Pe} = \frac{U^2 T_m}{\sigma_u^2 \tau_L} \qquad (9)$$

A value of 3 d is assumed for τ_L, consistent with the present simulations. Flow scenarios for which the

Peclet number exceeds 8 are denoted with the circled symbols in Fig. 10a–c (8 out of 64 cases). These correspond to the most egregious SSF outliers and represent cases with large mean flow, long PLD and small fluctuating current values, which will be atypical.

When the high Peclet number scenarios are neglected, estimates of regional self-seeding collapse nicely as a function of D_d/L for the 3 assumed values of L (Fig. 10d). Values of SSF are approximately 1 for D_d/L values less than ~0.3. For values of D_d/L greater than 0.3, regional-scale estimates of self-seeding decrease with increasing D_d/L following a power law relationship of approximately $(D_d/L)^{-1}$ (Fig. 10d).

These estimates of regional scale self-seeding fractions may prove useful for assessing the spatial scales needed to achieve the desired goals of marine protected areas. Estimates of SSF quantify the fraction of progeny produced at a point remaining within a region of size L as a function of the larval dispersal scale, D_d. Values of D_d can be determined from knowledge of flow statistics and an organism's PLD using the simple regression relationship presented in Table 1, or by empirical techniques (e.g. population genetics, natural microchemical tags). Quantitative estimates of regional-scale self-seeding can then be used to address the degree to which a given marine protected-area scenario achieves management objectives. For example, when the SSF is ~1, very little spillover of settlers will occur to neighboring sites. When SSF values are low, there may not be enough settled larvae to sustain recruitment of adults within the domain. By comparing SSF estimates from different organisms (with corresponding differing D_d values), assessments can be made of whether the designation of a particular marine protected area might act as a source and/or sink for settling larvae. Of course, full assessment of a marine protected area requires consideration of demographic factors such as mortality and fecundity and their density dependence, which is beyond the scope of the present manuscript.

The role of time

The present calculations of larval dispersal kernels are based on the superposition of many particle trajectories (N ≥ 5000), each of which can be thought of as ensuing from an independent larval release event. Kernel distributions estimated in this manner therefore represent ensemble mean dispersal patterns. Trajectories in the coastal ocean effectively reset themselves every ~3 d, as indicated by typical Lagrangian decorrelation timescales. Assuming continuous larval release, the present determinations of larval dispersal represent accumulated patterns for timescales of at least ~40 yr (based upon 5000 independent trajectories needed to produce a kernel distribution). Releases of propagules are generally not continuous through the year, and the kernel results may represent dispersal patterns integrated over even longer timescales, perhaps >100 yr.

For some applications, knowledge of larval dispersion on multi-decadal timescales is appropriate. These include considerations of genetic, physiological or behavioral adaptations that occur over the timescales of many generations. However, predicting annual stock-recruitment relationships of harvested marine organisms requires knowledge of larval dispersal over much shorter timescales. For the case of annual recruitment, the number of independent trajectories incorporated into a dispersal kernel will be less than 100 (~365 d/τ_L). Dispersion kernels constructed using 50 released larvae for the case of short (left) and long (right) PLD larvae in a typical flow field (U = 5 cm s^{-1} and σ_u = 15 cm s^{-1}) are shown in Fig. 11. A total of 12 and 13 out of 50 released larvae settled in this random sampling of the short PLD and long PLD cases, respectively. The solid lines are the result of the Gaussian fit to the modeled dispersal kernels (Fig. 4) found using 5000 released larvae. It is obvious that spatial patterns of settlement on short timescales will not follow 'nice' Gaussian distributions, but rather will represent discrete samples taken from the long-term ensemble distribution.

The discrete nature of annual kernels has major implications for predicting patterns of settlement, and thereby recruitment of sessile marine organisms on short timescales. Even if long-term ensemble dispersal patterns are predictable and stable, discrete sampling from kernel distributions will lead to stochastic variability in observed recruitment rates. This noise will make recruitment and/or larval settlement

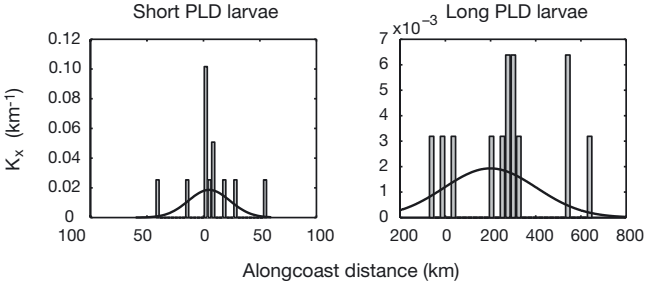

Fig. 11. Dispersion kernel constructed using a small number of released larvae for the case of short (left) and long planktonic larval duration (PLD) larvae (right) in a typical flow field (U = 5 cm s^{-1} and σ_u = 15 cm s^{-1}). A total of 12 and 13 out of 50 released larvae settled in these realizations of the short and long PLD larvae cases, respectively. Solid lines show results of the Gaussian fit to the simulated dispersion kernels (Fig. 5) found with 5000 synthetic larvae

datasets difficult to interpret and relate to oceanographic processes in a simple and general manner (e.g. Caffey 1985). Further, stochastic noise in recruitment rates due to random sampling of dispersal kernels can be expected to generate scatter in stock-recruitment relationships, with implications for the setting of policies for harvest of regulated marine species. In other words, on short timescales, larvae in the coastal ocean are 'stirred' and not 'well-mixed'. Settler distributions will exhibit 'well-behaved' patterns only when assessed over many independent realizations (e.g. Garrett 1983, Gabric & Parlsow 1994). A more complete discussion of the role of time on larval dispersal patterns is beyond the scope of this contribution, but these results highlight the importance of temporal scale in assessing larval dispersal and its role in several critical applications.

Acknowledgements. The authors would like to acknowledge support from NSF, NOAA and the Packard Foundation. Discussions with R. Warner, B. Kendall, C. Ohlmann, S. Airame, L. Washburn and J. Roughgarden were instrumental in the development of this work. T. Callendar helped in development of the simulation database. This is a contribution from the Santa Barbara Coastal LTER and PISCO programs.

LITERATURE CITED

Bauer S, Swenson M, Griffa A, Mariano AJ, Owens K (1998) Eddy-mean flow decomposition and eddy-diffusivity estimates in the Tropical Pacific Ocean. J Geophys Res 103: 30855–30871

Bird RB, Stewart WE, Lightfoot EN (2001) Transport phenomena, 2nd edn. John Wiley, New York

Black KP, Gay SG, Andrews JC (1990) Residence times of neutrally buoyant matter such as larvae, sewage or nutrients on coral reefs. Coral Reefs 9:105–114

Botsford LW, Moloney CL, Hastings A, Largier JL, Powell TM, Higgins K, Quinn JF (1994) The influence of spatially and temporally varying oceanographic conditions on meroplanktonic metapopulations. Deep-Sea Res II 41:107–145

Botsford LW, Hastings A, Gaines SD (2001) Dependence of sustainability on the configuration of marine reserves and larval dispersal distance. Ecol Lett 4:144–150

Brink KH, Beardsley RC, Paduan J, Limeburner R, Caruso M, Sires JG (2000) A view of the 1993–1994 California Current based on surface drifters, floats, and remotely sensed data. J Geophys Res 105:8575–8604

Caffey HM (1985) Spatial and temporal variation in settlement and recruitment of intertidal barnacles. Ecol Monogr 55:313–332

Cain ML, Milligan BG, Strand AE (2000) Long-distance seed dispersal in plant populations. Am J Bot 87:1217–1227

Cowen RM, Lwiza KMM, Sponaugle S, Paris CB, Olson BD (2000) Connectivity of marine populations: open or closed? Science 287:857–859

Davis RE (1985) Drifter observations of coastal surface currents during CODE. J Geophys Res 90:4741–4772

Dever EP, Hendershott MC, Winant CD (1998) Statistical aspects of surface drifter observations of circulation in the Santa Barbara Channel. J Geophys Res 103:24 781–24 797

Gabric AJ, Parslow J (1994) Factors affecting larval dispersion in the central Great Barrier Reef. In: Sammarco PW, Heron ML (eds) The bio-physics of marine larval dispersal. American Geophysical Union, Washington, DC, p 149–156

Garrett C (1983) On the initial streakiness of a dispersing tracer in two- and three-dimensional turbulence. Dyn Atmos Oceans 7:265–277

Gaylord B, Gaines SD (2000) Temperature or transport? Range limits in marine species mediated solely by flow. Am Nat 155:769–789

Hall CD (1975) The simulation of particle motion in the atmosphere by a numerical random-walk model. Quart J R Meteorol Soc 101:235–244

Hastings A, Higgins K (1994) Persistence of transients in spatially structured ecological models. Science 263: 1133–1136

Hill AE (1991) Advection-diffusion-mortality solutions for investigating pelagic larval dispersal. Mar Ecol Prog Ser 70:117–128

Jackson GA, Strathmann RR (1981) Larval mortality from offshore mixing as a link between precompetent and competent periods of development. Am Nat 118:16–26

Kinlan BP, Gaines SD (2003) Propagule dispersal in marine and terrestrial environments: a community perspective. Ecology 84:2007–2020

Ohlmann JC, Niiler PP, Fox CA, Leben RR (2001) Eddy energy and shelf interactions in the Gulf of Mexico. J Geophys Res 106:2605–2620

Okubo A (1971) Oceanic diffusion diagrams. Deep-Sea Res 18:789–802

Palumbi SR (2003) Populations genetics, demographic connectivity and the design of marine reserves. Ecol Appl 13 (Suppl):S146–S158

Possingham HP, Roughgarden J (1990) Spatial population-dynamics of a marine organism with a complex life-cycle. Ecology 71:973–985

Poulain PM (2001) Adriatic Sea surface circulation as derived from drifter data between 1990 and 1999. J Mar Sys 29:3–32

Poulain PM, Niiler PP (1989) Statistical analysis of the surface circulation in the California Current System using satellite-tracked drifters. J Phys Oceanogr 19:1588–1603

Richards SR, Possingham HP, Noye BJ (1995) Larval dispersion along a straight coast with tidal currents: complex distribution patterns from a simple model. Mar Ecol Prog Ser 122:59–71

Roberts CM (1997) Connectivity and management of Caribbean coral reefs, Science 278:1454–1457

Rodean HC (1996) Stochastic Lagrangian models of turbulent diffusion. Meteorol Monogrph Vol 26. Amer Meteor Soc, Boston, MA

Roughgarden J, Gaines S, Possingham HP (1988) Recruitment dynamics in complex life cycles. Science 241:1460–1466

Sammarco PW, Andrews JC (1988) Localized dispersal and recruitment in Great Barrier Reef corals: the Helix Experiment. Science 239:1422–1424

Scheltema RS (1971) Larval dispersal as a means of genetic exchange between geographically separated populations of shallow water benthic marine gastropods. Biol Bull 140: 284–322

Shanks AL (1995) Mechanisms of cross-shelf dispersal of larval invertebrates and fish. In: McEdward LR (ed) Ecology of marine invertebrate larvae. CRC Boca Raton, FL, p 323–368

Shanks AL, Grantham B, Carr MH (2003) Propagule dispersal distance and the size and spacing of marine reserves. Ecol Appl 13:S159–S169

Siegel DA, Deuser WG (1997) Trajectories of sinking particles in the Sargasso Sea: modeling of statistical funnels above deep-ocean sediment traps. Deep-Sea Res I 44:1519–1541
Slatkin M (1987) Gene flow and the geographic structure of natural populations. Science 236:787–792
Sundermeyer MA, Ledwell JR (2001) Lateral dispersion over the continental shelf: analysis of dye-release experiments. J Geophys Res 106:9603–9622
Swearer SE, Caselle JE, Lea DW, Warner RR (1999) Larval retention and recruitment in an island population of a coral-reef fish. Nature 402:799–802
Swenson MS, Niiler PP (1996) Statistical analysis of the surface circulation of the California Current. J Geophys Res 101:22631–22645
Thompson DJ (1984) Random walk modeling of diffusion in inhomogeneous turbulence. Quart J R Metorol Soc 110: 1107–1120
Thompson DJ (1987) Criteria for the selection of stochastic models of particle trajectories in turbulent flow. J Fluid Mech 180:529–556
Wellington GM, Victor BC (1989) Planktonic larval duration of one hundred species of Pacific and Atlantic damselfishes (Pomacentridae). Mar Biol 101:557–568
Wilson DJ, Sawford BL (1996) Review of Lagrangian stochastic models for trajectories in the turbulent atmosphere. Bound Layer Meteorol 78:191–210
Winant CD, Alden DJ, Dever EP, Edwards KA, Hendershott MC (1999) Near-surface trajectories off central and southern California. J Geophys Res 104:15 713–15 726
Wolanski E, Hamner WM (1988) Topographically controlled fronts in the ocean and their biological influence. Science 241:177–181
Wolanski E, Burrage D, King B (1989) Trapping and dispersal of coral eggs around Bowden Reef, Great Barrier Reef, following mass spawning. Cont Shelf Res 9:479–496
Wright S (1943) Isolation by distance. Genetics 28:114–138

Editorial responsibility: Otto Kinne (Editor), Oldendorf/Luhe, Germany

Submitted: September 6, 2002; Accepted: June 26, 2003
Proofs received from author(s): September 11, 2003